3
Memory Devices Based on Polymer-Small Molecule Blend

The first focus of the research work covered in this thesis is to fabricate and analyze the various properties, such as hysteresis, ON-OFF ratio, endurance and retention time of polymer-small molecule blend non-volatile memories. Polymer-based resistive memories are known to have switching properties [Lin *et al*., 2014]. Also, a conformational change in the small molecules is a well-known phenomenon which is responsible for the switching behavior of the organic molecular memories [Waser and Aono, 2007]. In this study, metal-insulator-metal (MIM) based devices with the active layer based on the combination of both polymer and small molecule have been explored. Devices with a blend of a small molecule 2,3-Dichloro-5,6-dicyano-p-benzoquinone (DDQ) and a polymer Poly(4-vinyl phenol) (PVP) were prepared and the combined effect of these two materials has been tested, and mechanisms of switching have been proposed in this study [Vyas *et al.*, 2016].

3.1 INTRODUCTION

Organic molecular memories have created a mark in the field of electronic devices in recent years. However, the lack of proper understanding of their switching mechanism is a big hurdle in their commercial realization. Currently, memory devices have a large share of the market of electronic devices. These are mostly conventional, silicon-based memory devices such as dynamic random access memory (DRAM), or flash memory. Both DRAM and flash are fast but they are expensive. Another problem with conventional silicon-based devices is that they are fabricated with a top-down approach, i.e. they are manufactured by patterning the bulk semiconductor into smaller devices. Molecular memories are manufactured by a bottom-up approach i.e. they are built with individual molecules. Hence, molecular memory devices have the potential of using a single molecule as the switching element [Chen *et al.*, 1999]. Apart from the capability of being a mono-molecular device, organic molecular memories also exhibit all the qualities of organic electronic devices like flexibility [Liu *et al.*, 2012], low cost [Tondelier *et al.*, 2004], solution processability [Chu *et al.*, 2005], and low switching power [Naber *et al.*, 2010].

There are many switching mechanisms available for the resistive memories. One of them is through a conformational change of the organic molecule present in the active layer of the MIM structure [Bandyopadhyay and Pal, 2004], in which the molecular geometry or the configuration of the electron cloud is altered to switch the conductivity of the device. Another method of resistive switching is due to blocking of charge carriers by immobile ions or space-charge [Scott and Bozano, 2007]. This electrostatic obstruction of charge is also termed as Coulomb blockade. Formation of conducting metallic filament is also a mechanism of increasing the conductivity of an insulating layer sandwiched between two metal layers. The metal filament formation is responsible for switching in some resistive memory devices [Cölle *et al.*, 2006]. Formation of charge transfer complex (CTC) has also been found to assist resistive switching in organic memory devices [Zhang *et al.*, 2016].

In this study, an organic non-volatile memory device has been fabricated with the blend of a polymer (PVP), and a small molecule (DDQ). The concentration of DDQ is varied with respect to that of PVP and their electrical and physical characterization were carried out. It was found that with the change in relative concentration of the small molecule in the blend, the ON-OFF ratio of the devices changes. The devices were found to exhibit two switching mechanisms which are metallic filament formation and conformational change. The variation in concentration causes

the change of the switching mechanism in the memory devices. It was found that at lower concentrations of DDQ in the blend, the filament formation dictates and at the higher concentrations of DDQ, the conformational change of DDQ is largely responsible for the switching.

3.2 EXPERIMENTAL SECTION

The memory devices with DDQ-PVP blend were made on the indium tin oxide (ITO) coated glass substrates. Memory devices were designed to have a crossbar architecture as shown in figure 3.1(a). To form a cross-bar architecture, substrates must have a thin strip of ITO over the glass. This was formed by etching of the ITO with the help of concentrated hydrochloric acid (HCl) and zinc dust. Scotch tape was used to protect the strip of ITO on the substrate.

To clean the substrates, the standard cleaning procedure (as discussed in Chapter 2) was followed. Substrates were first ultrasonicated in a soap solution. After a thorough cleaning in the soap solution, the substrates were rinsed in the deionized (DI) water multiple times to remove the traces of soap. After cleaning in the soap and rinsing in the DI water, the substrates were ultrasonicated for 15 minutes in acetone, DI water, and methanol each. The ultrasonication was repeated thrice for each solvent using a fresh supply of the solvent in every repetition. After the cleaning procedure was completed, the substrates were dried in a vacuum oven at 70°C for a few hours.

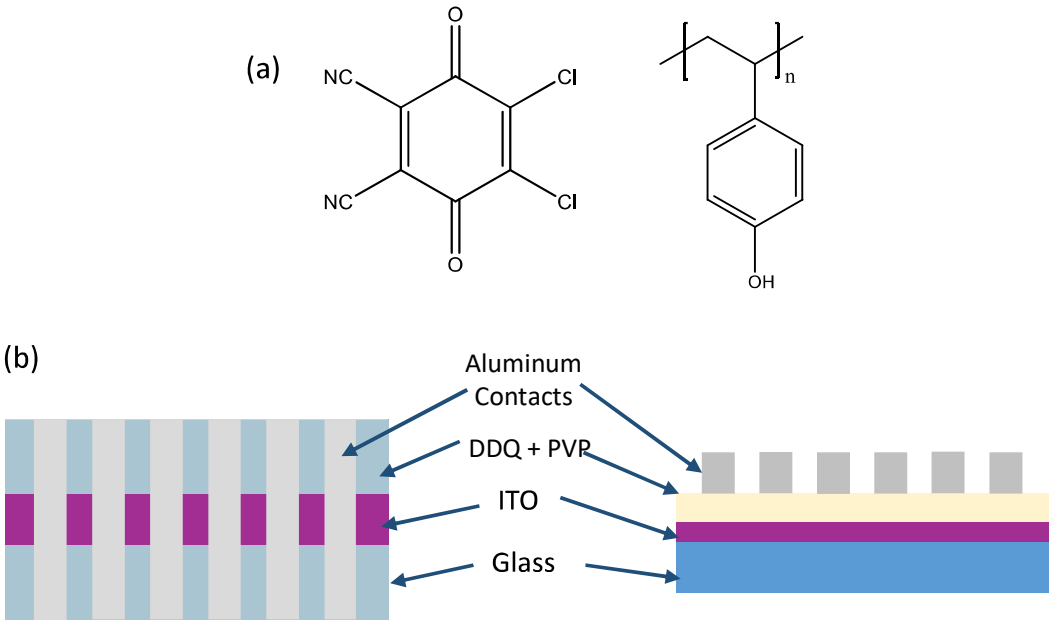

Figure 3.1: (a) Molecular structure of DDQ and PVP. (b) Schematic design of the metal insulator metal (MIM) memory devices based on DDQ-PVP blend

The materials used in the active layer were 2,3-Dichloro-5,6-dicyano-p-benzoquinone (DDQ) and Poly(4-vinylphenol) (PVP). The molecular structure of DDQ and PVP is shown in figure 3.1(a). Solution processing path was taken in the fabrication of the devices because of its simplicity. The solution of DDQ-PVP blend was prepared using isopropanol or isopropyl alcohol (IPA). All the chemicals were procured from Aldrich, Co., and were used without any further purification. The relative concentration of DDQ as a weight percentage of PVP was varied to fabricate different devices. The concentration of DDQ was varied from 5 wt. % of PVP, to 30 wt. % of PVP, with an increase of 5%, and another composition having DDQ as 50% weight ratio with respect to PVP. The solids DDQ and PVP were added to the solvent IPA, and the mixture was

ultrasonicated for a couple of minutes. These solutions were spin coated onto the substrates cleaned earlier at a rotational speed of 7400 rpm. These spin coated films were kept for drying in a vacuum chamber at room temperature for 12-14 hours. The ITO strip over the glass acts as the bottom electrode, over which the active layer was deposited. For top electrodes, a 70nm thick Aluminum layer was deposited with a thermal evaporation process using SC-Triaxis thermal evaporation system from Semicore. To create a crossbar architecture, a shadow mask was used having windows in form of thin stripes. The mask was placed on top of the active layer with the striped windows positioned perpendicular to the ITO strip.

After depositing the active layers, the thickness measurement was carried out with the help of surface profilometry using Bruker Dektak, XT-100 profilometer. To find out the thickness using a profilometer, a step was created by etching out a portion of the active layer. The average thickness in these devices was found to be 174 nm. Surface morphology of the thin films was characterized by atomic force microscopy using Park System's XE-70 SPM system. The electrical characterization of the devices has been carried out in a vacuum chamber by two probe method, using Keithley 6430 sub-femtoampere source meter controlled by custom LabView programs in a computer. The UV-visible absorbance spectra were examined for possible diagnosis of a charge transfer complex (CTC). For reference, individual spectra of PVP and DDQ was also recorded along with the different combinations with IPA being used as the solvent.

3.3 RESULTS AND DISCUSSION

3.3.1 Absorbance

Absorbance spectra of pure DDQ, pure PVP and different combinations of the two is shown in figure 3.2. As observed from figure 3.2, the absorbance peak of only DDQ in IPA is observed at 349 nm whereas, for PVP, the absorbance peak lies in the ultra-violate (UV) region. For combination, as the concentration of the DDQ increases, the height of the DDQ peak also increases proportionately. However, there is no hint of peak shifting or introduction of new peaks in the absorbance spectra which signifies that there are no charge transfer complexes formed in the combination of DDQ and PVP. The absorbance was also measured over the thin films and no evidence of charge transfer complexes was found there either.

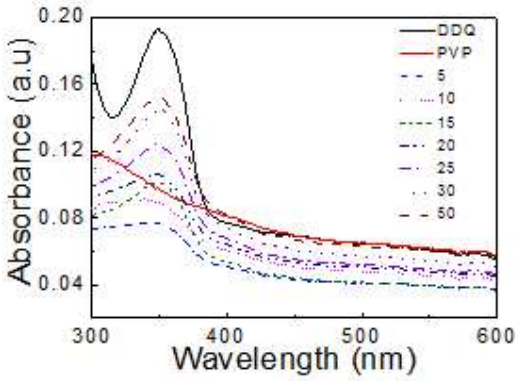

Figure 3.2: Absorption spectra of pristine DDQ and PVP and mixtures of both at various concentrations (5% - 30% with a 5% increase of DDQ in PVP and 50% of DDQ in PVP) in IPA

3.3.2 Surface Morphology

The surface morphology of the organic thin films was studied with Park System's atomic force microscope (AFM). Characterization was carried out in the non-contact mode with a soft-tapping cantilever to prevent the organic molecules from sticking to the cantilever. A scan rate of at least 0.25 nm^2/s was used to extract a high resolution of the images. The AFM images for all

samples are as shown in figure 3.3. The films deposited for AFM characterization were fabricated under the same conditions as the final devices.

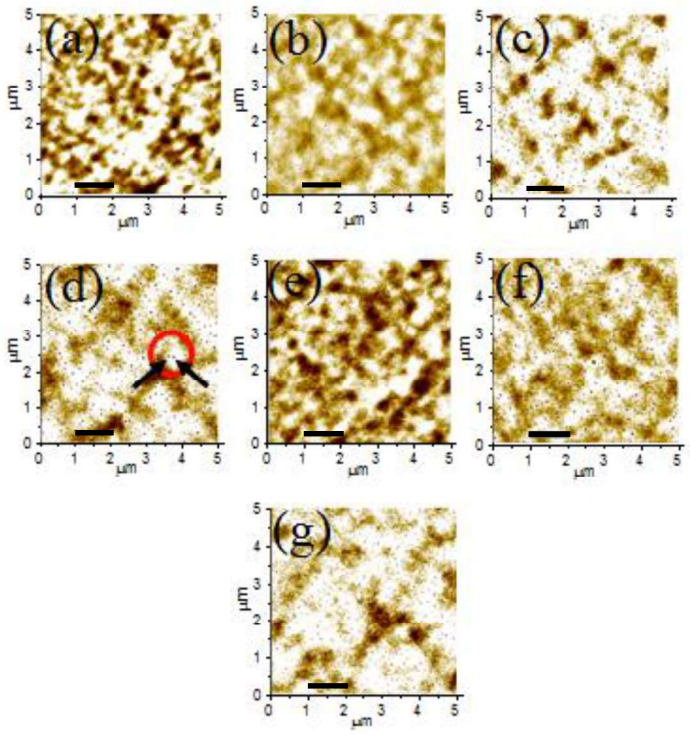

Figure 3.3: AFM images of DDQ and PVP having (a) - (g) 5%, 10%. 15%, 20%, 25%, 30%, and 50% of DDQ (w/w) with respect to PVP. The scale bars show a distance of 1 μm.

It is found that apart from the apparent roughness, all films contain small pinholes. The dimensions of the pinholes are as follows. The number of pinholes per 25 μm^2 scan area in devices with 5% DDQ concentration was 231 and the size of the pinholes ranged from 20 – 120 nm. As with the device having 10% DDQ concentration, the number of pinholes was 430 and the size of the pinholes ranged from 35 to 85 nm. For the device with 15% concentration, there were 586 pinholes ranging from 25 to 90 nm in size. For 20% concentration device, 438 pinholes with the size of 20-100 nm were observed. The 25% concentration device had 430 pinholes with 20-55 nm size. For 30% devices, the number of pinholes was 426 and the size ranged from 30 to 95 nm and for 50% it was 532 in number with size varying from 25 to 85 nm. An oscillatory behavior in the number of pinholes was observed with increasing concentration. The reason for this behavior is a subject of investigation.

3.3.3 Electrical Characterization

The devices with DDQ concentration of 5%, 10%, 15%, 20% 25%, 30% and 50% are labelled as A, B, C, D, E, F, and G respectively. As discussed earlier, the devices were scanned in a vacuum chamber with two probe method. The voltage sweep program was used to find out the I-V response of the devices. The slew rate or the rate of change of voltage was 50 mV/s. The I-V characteristics of the devices A to G are as shown in figure 3.4. For device A, as shown in figure 3.4 (a), the ON (high conductance) and OFF (low conductance) currents in the positive half cycle have a larger difference. In the negative half of the sweep, the ON and OFF state currents have smaller differences. The largest value of the ON-OFF ratio recorded for this device in the negative direction is 5. This value is not sufficiently high for a typical memory device. The ON-OFF ratio in the positive half though is 32. The sweep voltage range was varied up-to 4V, but not very significant change in the performance was observed.

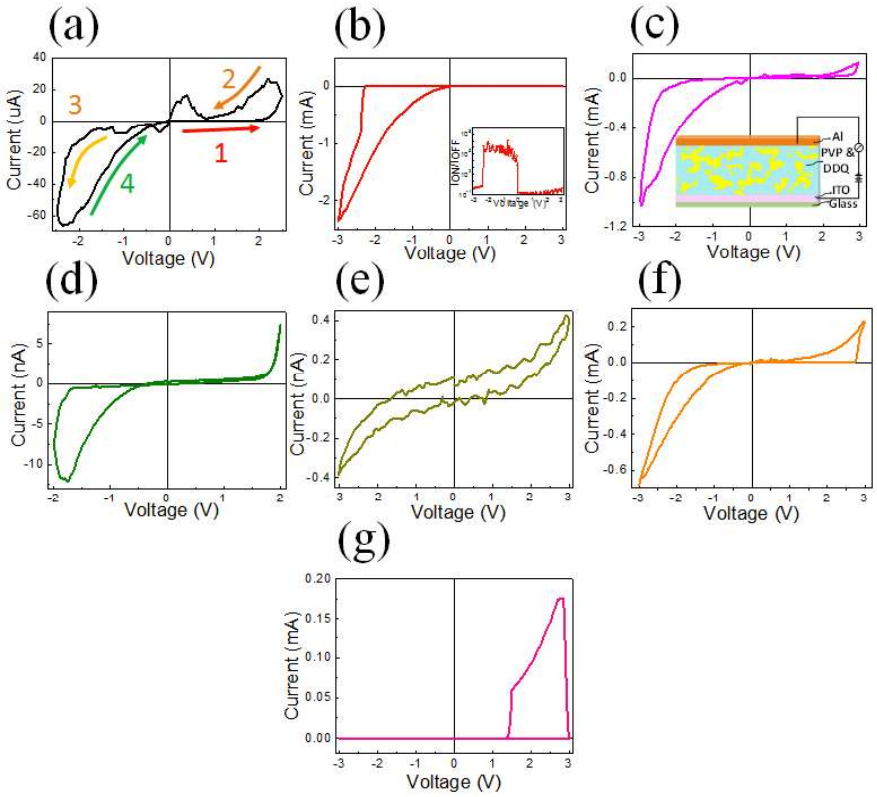

Figure 3.4: (a) IV characteristic curve of device A. The numbered (1 to 4) arrows (red, orange, yellow, and green) represent the sequence of scanning. (b) and (c) IV characteristic curves for devices B and C, scanned from 3 to -3V. The inset of (b) shows the ON-OFF ratio for the device within the spectrum of the above voltage scan and the inset of (c) shows the polarity of the I-V characterization scheme. (d)–(g) The IV characteristic curves of devices D, E, F, and G.

The maximum ON-OFF ratio observed for device B, was 10^6 as can be seen from the inset in figure 3.4(b). The IV curve, in this case, is a lot smoother than the device A. It indicates that the conduction is not jittery anymore, means the pathway for the conduction is firmer in this device. For device C, the maximum ON-OFF ratio observed in the negative direction was 150 which is significantly less than that of device B. In positive direction though, there is no hysteresis, i.e. there is no switching.

As shown in figure 3.4(e) device E showed an IV curve which was not smooth, also the ON-OFF ratio observed was on the lower side – 23 in the negative bias and 135 in the positive bias. Overall current in this device is significantly lower than that of device D. Overall the current density in the device was low showing a very poor conduction. Although some devices showed switching in the positive direction consistently, the occurrence of switching was relatively very low compared to the instances where switching did not occur. This situation indicates a possibility of space-charge accumulation of charge carriers, which occasionally releases the charge carriers in bulk which causes the switching. This is an indication that DDQ has become the deciding factor in the switching mechanism.

For device F, the highest ON-OFF ratio is approximately 10 in negative bias whereas in the positive direction it was 10^4. There was hardly any difference in the ON and OFF currents in the negative voltage scan in device G. However, in the positive voltage scan, the highest ON-OFF current ratio was of the order of 10^6. This ON-OFF ratio is a steep jump from the previous two

devices. Furthermore, the devices with 50% DDQ concentration (G), showed reproducibility consistently in many scans.

3.3.4 Switching Mechanism

It can be clearly observed from all the IV characterization of all the devices that the ON-OFF ratio and direction of switching vary in a distinctive pattern with concentration. Switching started in the negative bias with a low ON-OFF ratio. The ON-OFF ratio that increases up to 10^6 which then starts decreasing as the concentration increases. At one point, the ON-OFF ratio comes to a very low value, and then the polarity of switching changes to the positive direction. Then in the positive direction, as the concentration increases, the ON-OFF ratio again increases and reaches 10^6. It is known that inherently DDQ based MIM devices show switching in positive voltage scan [Bandhopadhyay and Pal, 2003]. However, the switching in the negative side of the voltage scan suggests another mechanism i.e. the metal filament formation [Jakobsson *et al.*, 2007; Stewart *et al.*, 2004]. The metal filament is formed due to the electromigration of aluminum (Al) ions through the pinholes present on the surface of the active layer. Due to the external electric field, Al ions are forced to move through the pinholes which make the conduction better. When this filament reaches to the bottom of the active layer i.e. to the ITO electrode, the conduction is very high as can be seen in figure 3.5 (a) blocks 1 to 3. Because of the low concentration, it can be safely said that only a small portion of pinholes is filled with the DDQ molecules. Therefore, the filament formation is the only mechanism responsible for switching of the conductance. With the increase in concentration, the pinholes are mainly filled with the DDQ molecules. The switching therefore mainly depends on the conformational changes of DDQ. Hence the ON-OFF ratio of the device with high DDQ concentration increases significantly as can be observed in figure 3.5 (a) block 4 and 5.

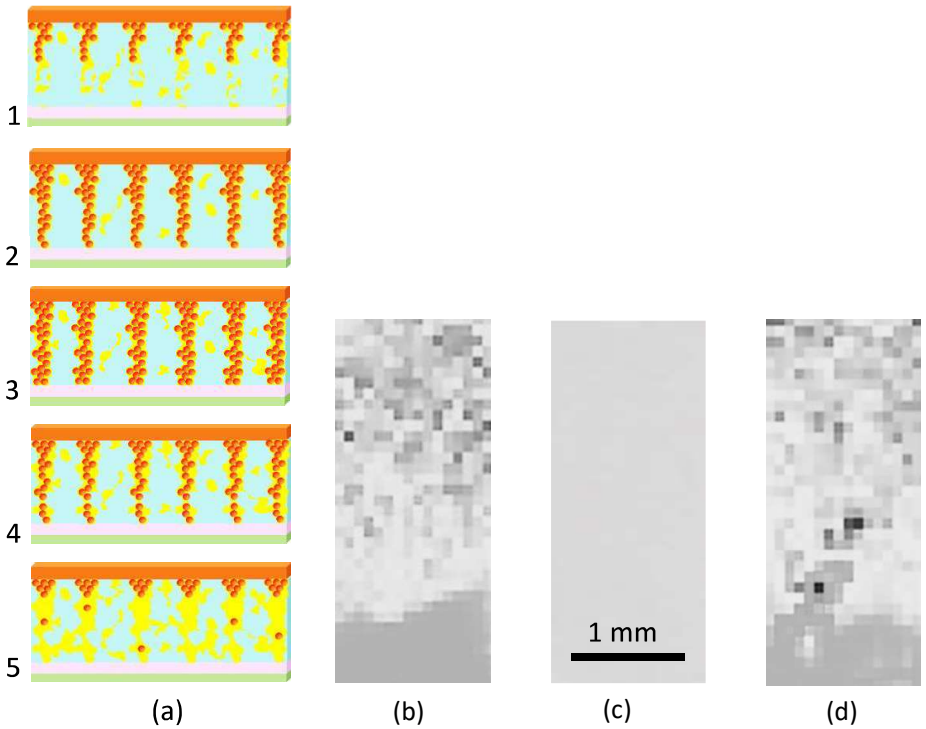

Figure 3.5: (a) Schematic of conduction mechanism in the devices showing formation of the aluminum filament at lower DDQ concentration and conformational change of DDQ at the higher concentration. The yellow region represents parts of DDQ, the light blue region is PVP matrix, and the orange color balls represent Al ions. (b)-(d) IR images of top Al electrode while a bias voltage of -3V, +3V and -3V is applied respectively.

Because PVP is an insulator, it has a high band gap as compared to DDQ hence the Al ions are propelled due to the interaction between Al ions and the polymer. However, the interaction between the DDQ and Al causes the switching to occur in the positive direction as observed in the higher concentration devices. In a negative bias, DDQ is reduced by capturing all the electrons drifting through the Al by the electronegative oxygen atoms present in DDQ. It releases the electrons under appropriate applied positive bias, which causes a steep rise in conductance in the positive bias.

The formation of the filament was confirmed by infrared (IR) imaging of the top of aluminum electrodes during the negative voltage scans as shown in figure 3.5 (b)-(d). Panel (b) shows the IR image at -3V and as clearly shown the filaments through the random distribution of pinholes through the black spots. Panel (c) is the IR image of the same cell when the voltage was reversed and panel (d) is again when the cell is applied -3V. Because of the low resolution of the IR camera (Cedip (FLIR)-JADE-MW) the images are pixelated, but the filament formation is clearly observed.

3.3.5 Endurance and Retention Time Measurements

The endurance of all the devices was tested, and all the devices found to be fairly repeatable. To test the endurance of the devices, a write voltage pulse was applied for some time, and then the device was scanned with a relatively low voltage – read voltage pulse which was followed by an erase voltage pulse and then a probing of the device by read voltage pulse was carried out again. The sequence of Write-Read-Erase-Read voltage pulses is applied many times to test the repeatability and reliability of the devices. In figure 3.6 (a), the scan for endurance is shown for a device where the write voltage (V_{write}) is -3V, the erase (V_{erase}) voltage is +3V, and the read voltage (V_{read}) is -0.5V. The erase and write pulses' duration were 5s and the read voltage was applied for 20s followed by a write or erase pules. The train of this sequence was applied for 1000s (20 cycles) and the memory devices were found to be stable during that cycle. The current levels during the read cycle do not change significantly hinting towards the stability even during the random probe of the devices.

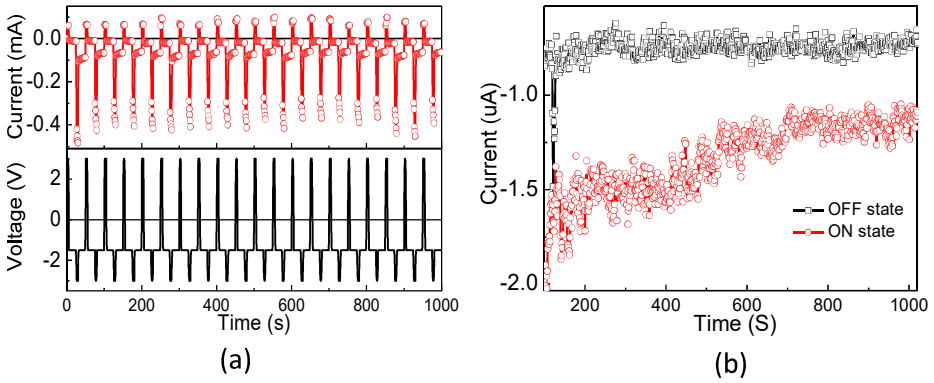

Figure 3.6 (a) The endurance test: write-read-erase-read sequence to test the consistency of reading the written and erased states which are written at -3 V, and erased at 3 V. (b) Retention study of device: After writing and erasing by -3 V (ON state) and 3 V (OFF state) respectively, the states are read for 1000 s.

For the retention time studies, the devices were scanned using a small read voltage for a long time after being subjected to a write or erase voltage for a short time duration as shown in figure 3.6 (b). The write, erase, and read voltage values in the retention scan were -3V, +3V, and -0.5V respectively. The read voltage was applied for more than 1000s and it was found that the

currents stayed reasonably stable in the entire period of probe voltage. Retention properties are useful in the ROM applications of the device whereas endurance tests are a test of device's RAM properties. The devices were observed to show both RAM and ROM properties in these scans.

3.4 CONCLUSION

To sum up, the non-volatile memory devices were fabricated using a polymer-small molecule blend. The ON-OFF ratio for the devices was tuned by varying the concentration of DDQ with respect to the PVP in the blend. The ON-OFF ratio was found to be high when the DDQ concentration with respect to the PVP is either very low or relatively high (50%) with respect to that of PVP. When the concentration of DDQ is less, the switching is observed in the negative bias direction. When the weight ratio of DDQ and PVP is half, the bistability is observed in the positive bias voltage. This phenomenon can be explained by two separate switching mechanisms – metallic filament formation and conformational change of the small molecule. Both of them are verified by AFM images where the small pinholes were observed on top of the active layer. Hence, the ON-OFF ratio and the direction of switching can be tuned with the concentration of small organic molecule in the polymer matrix.